ADVANCED FUNCTIONAL MATERIALS

Single and Multiple-Step Dip-Coating of Colloidal Maghemite (γ-Fe_2O_3) Nanoparticles onto Si, Si_3N_4, and SiO_2 Substrates**

By *Tae-Sik Yoon*, *Jihun Oh*, *Sang-Hyun Park*, *Viena Kim*, *Byung Gil Jung*, *Seok-Hong Min*, *Jongnam Park*, *Taeghwan Hyeon*, and *Ki-Bum Kim**

The adsorption behavior of colloidal maghemite (γ-Fe_2O_3) nanoparticles, passivated by oleic acid and dispersed in octane solution, onto three different substrates (Si, Si_3N_4, and SiO_2) is investigated. The average nanoparticle size is 10 nm, with a size variation (σ) less than 5 %. The adsorption of particles is strongly dependent on both the type of substrate and the particle concentration in solution. By a single-dipping process, we have obtained a maximum coverage of 0.45 on a Si substrate, but much less on other substrates (0.19 on Si_3N_4 and 0.14 on SiO_2). The particle coverage was drastically increased by the multiple-adsorption process, where the process of dipping and drying was repeated multiple times. With this process, we can obtain a maximum particle coverage of about 0.76 on a Si substrate and 0.61 on a thermally grown SiO_2 substrate.

1. Introduction

The demonstration of unique electrical,[1,2] optical,[3,4] and magnetic[5,6] properties of nanoparticles, and the feasibility of making a variety of functional devices utilizing these particles, have attracted intense interest. As a result, one has witnessed the development of various methods specifically aimed at the formation of nanometer-size particles and wires with uniform size distributions.[7–12] Among these, the wet-chemical synthesis of colloidal nanoparticles stabilized by surfactant molecules appears to be one of the most promising methods for making particles less than 10 nm in size with a narrow size distribution.[12–16] Moreover, the demonstration that these colloidal nanoparticles form two- or three-dimensionally ordered close-packed assemblies upon evaporation of the solvent suggests a strong possibility for making functional devices out of these particles.[12–16]

[*] Prof. K.-B. Kim, Dr. T.-S. Yoon, J. Oh, S.-H. Park, V. Kim
NANO Systems Institute
School of Materials Science and Engineering
Seoul National University
Seoul 151-742 (Korea)
E-mail: kibum@snu.ac.kr

B. G. Jung, Prof. S.-H. Min
Department of Metallurgical Engineering
Kangnung National University
Kangnung 210-702 (Korea)

J. Park, Prof. T. Hyeon
School of Chemical Engineering
Seoul National University
Seoul 151-744 (Korea)

[**] The authors are grateful to Prof. Soo Young Park, Prof. Jang-Joo Kim, and Dr. Jeffrey F. Webb at Seoul National University for helpful discussions. This experiment was carried out using the facilities in the Research Institute of Advanced Materials at Seoul National University. The authors are grateful for a Brain Korea 21 scholarship from the Ministry of Education, Korea. This work was supported by the Korea Research Foundation Grant (KRF-2002-042D00077).

While the self-assembly behavior of these particles has been fully demonstrated, it remains a challenge to deliver and assemble those particles on a wafer scale substrate. Indeed, this should be resolved to make any kind of functional device employing these particles. In order to accomplish this objective, researchers have tried various processes, including Langmuir–Blodgett,[17–20] spin-coating,[21–23] and adsorption by dip-coating[24–31] methods. However, each of these processes has some advantages and disadvantages, and none of these has been successful with large size substrates. The Langmuir–Blodgett method, while having the best results so far with respect to large-area self-assembly, still has the problem of crack formation after the drying process, and is known to be a difficult process for delivering particles onto a non-planar or a patterned substrate. Spin-coating also faces difficulties in delivering an exact amount of particles onto a substrate, as well as difficulties in delivering particles onto a non-planar substrate or a patterned wafer.

On the other hand, the simple adsorption process of the dip-coating method offers many advantages. A self-limited monolayer of particles can be deposited because the adsorption process occurs by the interaction between the particle and substrate, and particles can be delivered onto planar, non-planar, and patterned substrates. Moreover, one does not have to worry about wasting particles. For instance, Sato et al. formed 20 nm size Au particles coated with citrate ions, causing the particles to become negatively charged. The particles were then delivered onto a SiO_2 substrate using the dip-coating method employing an amino-functionalized silane, [3-(2-aminoethylamino)propyl]trimethoxysilane, as an adsorption agent.[24] The affinity of this adsorption agent immobilizes the Au particles on the substrate, and the repulsive force between negatively charged particles prevents them from aggregating or piling up on top of each other. However, the density of particles was about 1×10^{11} cm^{-2}, corresponding to a coverage of about 0.35. The coverage was defined as the ratio of the number of adsorbed particles on the substrate to the theoretical maximum number of close-packed particles on the substrate. Grabar et al. also used citrate Au particles, and formed a parti-

 © 2004 WILEY-VCH Verlag GmbH & Co. KGaA, Weinheim DOI: 10.1002/adfm.200305088 *Adv. Funct. Mater.* **2004**, *14*, No. 11, November

cle layer on a substrate coated with an organosilane as an adsorption agent.[25] However, when the charged particles adsorbed onto the substrate, they reached a coverage less than 0.3 due to the Coulombic-repulsive interaction between charged particles.[24–26] Also, Feder and Giaever reported the adsorption of ferritin molecules on polycarbonate and carbon surfaces.[27] They showed that the coverage of ferritin was limited by the random sequential-adsorption problem, where the maximum coverage is less than 0.55.[27,32]

In order to overcome these limitations, the layer-by-layer adsorption process has been used to increase the particle coverage by alternately repeating the adsorption of the glue layer (composed of materials such as electrolytes) and the particle layer.[28,29] For instance, Kotov et al. have shown that negatively charged and surfactant-stabilized CdS, PbS, and TiO_2 particles adsorb on a positive electrolyte, facilitated by the strong electrostatic interaction.[28] In addition, Sun et al. employed polymer-mediated layer-by-layer adsorption by using polyethylenimine (PEI) to form a FePt particle layer passivated by an oleic acid/oleylamine surfactant.[29] Through the exchange of surfactant around the particle with PEI attached to substrate, the PEI and FePt particle layer was alternatively adsorbed onto substrate. Though this process seems to be successful for forming dense particle-assembly structures, the monolayer coverage was shown to be still limited. The limited coverage in this process was due to the strong interaction between particles and the glue layer, which immobilizes the particles.

In addition, Tilley and Saito have recently reported the adsorption of Au particles onto a chemically modified Si surface.[31] They investigated the effect of surface polarities and the pulling rate of the substrate during the dip-coating process on the adsorption of Au particles passivated by a dodecanethiol surfactant and dispersed in hexane. The particle coverage could be varied from 0.05 to 0.95 by changing the surface polarity of the substrate. The maximum coverage was obtained on the most hydrophobic surface at the lowest pulling rate of 40 $nm\,s^{-1}$. However, they measured the areal coverage using scanning electron microscopy images of the assembled particles, including the non-close-packed area as well, which may have resulted in an inaccurate estimation of coverage. Also, the low pulling rate required to obtain the highest coverage may present practical problems.

In this study, we investigate the adsorption of 10 nm-diameter γ-Fe_2O_3 nanoparticles, sterically stabilized by oleic acid surfactant and dispersed in octane solvent, onto Si, Si_3N_4, and SiO_2 substrates without any chemical modification of the substrate surface as we try to understand some of the fundamental limitations of the simple adsorption process. Then, to overcome these limitations, we suggest a multiple-adsorption process by repeating the sequence of dipping and drying processes without employing any glue layer. We will then show that the particles can be delivered with a maximum coverage of 0.76 onto Si and 0.61 onto SiO_2 substrates.

2. Results and Discussion

2.1. The Case of a Single-Adsorption Process

Figure 1 presents plan-view transmission electron microscopy (TEM) bright-field images of nanoparticle assemblies at nanoparticle concentrations of 0.24, 4.9, and 29×10^{13} cm^{-3}, on hydrogen-terminated Si (Figs. 1a–c), Si_3N_4 (Figs. 1d–f), and SiO_2 substrates (Figs. 1g–i). Most of the particles adsorbed on the substrate are present as monomers or dimers at the low concentration of 0.24×10^{13} cm^{-3} (Figs. 1a,d,g). On the other hand, as the particle concentration is increased, the particles tend to assemble at certain areas on all three substrates (center and right columns of Fig. 1). The randomly oriented small assemblies, especially, tend to connect with each other on the Si

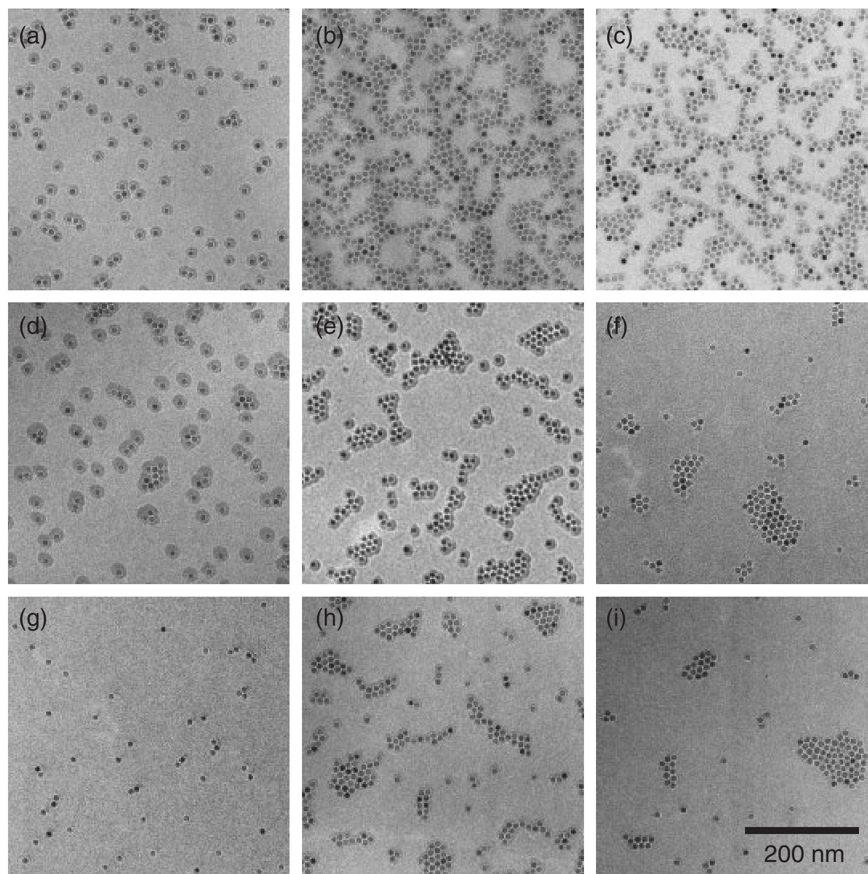

Figure 1. Plan-view TEM bright-field images of γ-Fe_2O_3 nanoparticle assemblies obtained from solutions with concentrations of 0.24, 4.9, and 29×10^{13} cm^{-3} on a–c) hydrogen-terminated Si, d–f) Si_3N_4, and g–i) SiO_2 substrates.

© 2004 WILEY-VCH Verlag GmbH & Co. KGaA, Weinheim

substrate. The coverage of particles as a function of concentration is presented in Figure 2. The coverage increased up to 0.45 on Si, 0.19 on Si_3N_4, and 0.14 on SiO_2 substrate as the concentration is increased, and then gradually decreased on all substrates as the particle concentration in the solution increased further. The coverage values less than 0.5 seem to correspond with the results reported by Feder and Giaever,[27] where the coverage is limited by the random sequential-adsorption problem. Also, the coverage on Si and SiO_2 substrates are similar to those reported by Tilley and Saito.[31] It should be noted that the wetting properties of the solution is quite important: a non-wetting solution will result in nonhomogeneous adsorption of nanoparticles. Truong and Wayner have theoretically calculated the equilibrium profile of an octane solution horizontally wetting Si and SiO_2 substrates.[33] They noted that the wetting profile is determined by the capillary and van der Waals' dispersion forces, and experimentally observed that the octane solution wets both substrates well.

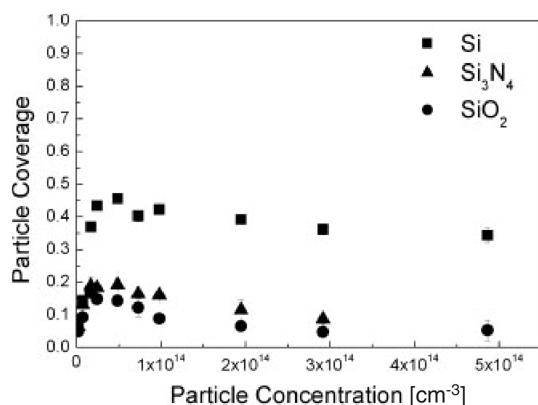

Figure 2. Particle coverage as a function of concentration on each substrate.

From the results shown in Figures 1,2, we note the following. First, the particle coverage is clearly dependent on the type of substrate. The thickness of the solution layer that clung to the substrate after withdrawing the substrate from solution was calculated to be ~0.3 μm using the Landau–Levich equation,[34] and using the viscosity, density, and surface energy data of pure octane solvent.[35] The number of particles in this layer corresponds to a coverage <0.02 even at the highest concentration in this experiment. Therefore, the contribution of particles in the solution which clung to the substrate during pulling-out can be neglected. It should be noted that this calculation may not be exact, since the viscosity, density, and surface energy data of pure octane solvent will be different from those of the colloidal solution. However, it still indicates that the coverage due to the particles in the solution seems to be negligible. Rather, the substrate-dependent coverage seems to be due to the adsorption driven by the interaction between particle and substrate, which depends on the substrate.[15,27–31,36] Also, although the particle coverage increases with the particle concentration in the solution, the experimentally observed coverage can not be explained by a simple Langmuir adsorption: it does not increase to the level of monolayer coverage with increasing particle concentration. On the contrary, there is a maximum attainable coverage for each substrate.

To understand the coverage dependence on the substrate, we have considered the interactions between the particle and the substrate affecting particle adsorption. One interaction is the van der Waals' attractive interaction between the particle and substrate.[15,30,36] The strength of the van der Waals' interaction is proportional to the Hamaker constant.[15] The material-dependent Hamaker constant A for the γ-Fe_2O_3/octane/substrate system can be expressed as[36]

$$A \approx \left(\sqrt{A_{\mathrm{sub}}} - \sqrt{A_{\mathrm{octane}}}\right)\left(\sqrt{A_{\gamma\ \mathrm{Fe_2O_3}}} - \sqrt{A_{\mathrm{octane}}}\right) \quad (1)$$

where A_{sub}, A_{octane}, and $A_{\gamma\text{-}\mathrm{Fe_2O_3}}$ are the Hamaker constants of the substrate, octane, and γ-Fe_2O_3 nanoparticles, respectively. The Hamaker constants of each substrate are 1.59 eV,[37] 1.04 eV,[38] and 0.41 eV[38] for Si, Si_3N_4, and SiO_2, respectively. Those of octane and the nanoparticles are 0.28 eV[34] and 2.59 eV, respectively (see Appendix). Therefore, the Hamaker constants $A = 0.79$ eV for when the substrate is Si, 0.53 eV for Si_3N_4, and 0.12 eV for SiO_2 correlate with the experimental results, at least qualitatively, with the highest coverage on the Si substrate and the lowest on the SiO_2 substrate. Since the adsorption takes place within the solvent, we calculated the interaction energies using the solvent as a medium rather than the surfactant.[30] In addition, Tilley and Saito have shown that systems consisting of nonpolar thiol-coated Au particles and chemically modified Si substrates have different particle coverages, depending on the surface polarities of the modified Si substrate.[31] They modified the surface polarities to have water contact angles from ~10 to 100°, and found that the thiol-coated Au particles adsorb with the highest coverage on the most hydrophobic substrate. This matches our results that show the highest coverage of oleic acid-coated γ-Fe_2O_3 particles occurs on the most hydrophobic Si substrate. However, the coverage could not be quantitatively correlated with the interactions on each substrate, due to the complicated adsorption behavior which does not follow a simple Langmuir isotherm, as shown in Figure 2. Also, the contributions of van der Waals' interactions and the substrate surface polarity to particle coverage are not yet fully understood.

In order to explain the observed increase of coverage with concentration to a maximum, followed by a gradual decrease at higher concentrations, one has to consider another competing mechanism which hinders the adsorption of particles. Here, we suggest that both of these phenomena are due to the adsorption of freely dispersed surfactant (oleic acid) on the substrate. The colloidal solution has been prepared by dissolving a known amount of the particle powder consisting of particles and surfactant. The number ratio of surfactant molecules to particles in the powders was found to be ~6500:1 using inductively coupled plasma atomic emission spectroscopy (ICP-AES) elemental analysis; similar to the number obtained by Fried et al.[39] If one assumes that all the surfactant molecules adsorb onto particles, the adsorbed surface area per surfactant

 © 2004 WILEY-VCH Verlag GmbH & Co. KGaA, Weinheim

on the particle is approximately 5 $Å^2$. This number is much smaller than the reported value, ~25 $Å^2$, of adsorbed area per surfactant when oleic acid forms a close-packed monolayer.[39,40] Therefore, one can assume that an abundance of freely dispersed oleic acid molecules exist in the solution, and that their concentration should also be linearly proportional to the particle concentration in solution. It is also assumed that these oleic acid molecules may also adsorb onto the substrate, and that these adsorbed surfactants may reduce the interaction energy between the particle and the substrate, or even fully prohibit the adsorption of particles, and thereby decrease the number of adsorption sites. The effect of oleic acid on the particle coverage has been identified by the following experiments. First, the particle coverage was found to drastically decrease, from ~0.45 on the hydrogen-terminated Si substrate, to ~0.27 on the Si substrate coated with a layer of oleic acid formed by immersing the hydrogen-terminated Si substrate in oleic acid solution before particle adsorption. Second, it was observed that particle coverage on the SiO_2 substrate drastically decreased, from ~0.17 to ~0.02, when we added an excess of oleic acid, increasing its concentration to $\sim 1.1\times10^{-6}$ mol cm^{-3} in the colloidal solution. These results indicate that excess oleic acid may adsorb on the substrate and decrease the particle coverage. Therefore, the competitive adsorption behavior determines the particle coverage, with a maximum coverage at a certain concentration, and gradual decrease with further increase in particle concentration dependent on the various kinetic parameters of the involved adsorbates (particle and oleic acid).

One also has to consider the effect of the jamming limit when considering the adsorption of these particles in the solution. The jamming limit occurs during the random sequential-adsorption process when particles adsorb as monomers randomly and irreversibly, and are immobilized after adsorption. Then, the non-adsorbed area becomes too narrow for nanoparticles to adsorb on, as illustrated in Figure 3a. Therefore, a submonolayer eventually forms, with a maximum area coverage of about 0.55.[27,32] Since colloidal particles adsorb randomly on surfaces as monomers, and there appears to be no aggregation between the particles in the solution, it is reasonable to apply the jamming limit in this case.[41] However, the jamming limit may not be exactly 0.55, since the particles can migrate on the substrate or desorb reversibly from the substrate.[27] No matter what the exact jamming limit is, the random sequential-adsorption problem eventually results in sub-monolayer coverage.

2.2. The Case of a Multiple-Adsorption Process:

Up to now, we have shown that nanoparticles are placed on the substrate via adsorption by dipping the substrate in a colloidal solution. However, the maximum coverage of particles is below 0.5, even in the case of Si substrate. In addition, considering the random sequential adsorption of particles, it is more or less clear that producing a monolayer coverage of particles on the substrate by the simple dipping process is not an easy matter. In order to increase the coverage beyond the limit set by the random sequential-adsorption problem, we suggest a multiple-adsorption process: the process of dipping and drying the solvent after withdrawing the substrate from solution is repeated. During the first adsorption step, nanoparticles adsorb on the substrate in the solution as monomers,[41] schematically illustrated in Figure 3a. After evaporation of the solvent, these monomers form assemblies by the interactions between particles, and the non-adsorbed area becomes large enough for nanoparticles to adsorb, as depicted in Figure 3b. In addition, the energy state of assembled nanoparticles might be different than those of monomers. It is assumed that these assembled nanoparticles are more stable compared with the monomer particles due to the interactions between particles. Thus, the nanoparticle concentration on the substrate in the steady state will be increased. In this case, the coverage will be dependent on the adsorption probability (coverage resulting from a single adsorption step), the number of adsorption steps (dipping the substrate followed by drying the solvent), and the stability of the preformed assembly in solution at the following the adsorption step. A multilayer is not expected to form, even with multiple-adsorption steps, because the surfactants encapsulating the nanoparticles prevent them from adsorbing onto nanoparticle assemblies in solution. The inter-particle interaction energy in solution was calculated using the van der Waals' attractive interaction energy and the steric repulsion interaction energy.[42] This calculation results in a small interaction energy, about 0.02 eV, which is similar to the thermal energy at room temperature, so the particles are stable without aggregation in the solution and do not form a multilayer on the substrate.[43]

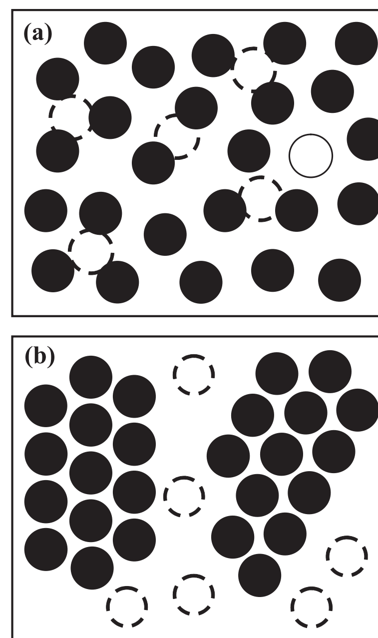

Figure 3. Schematic illustration of adsorption of nanoparticles onto substrate a) as monomers before solvent evaporation, and b) as assemblies after solvent evaporation.

The plan-view TEM bright-field images of the γ-Fe_2O_3 nanoparticle assemblies produced with number of dipping steps $n = 1$, 5, 10, and 15 times are shown in Figure 4 (on Si substrate)

 © 2004 WILEY-VCH Verlag GmbH & Co. KGaA, Weinheim

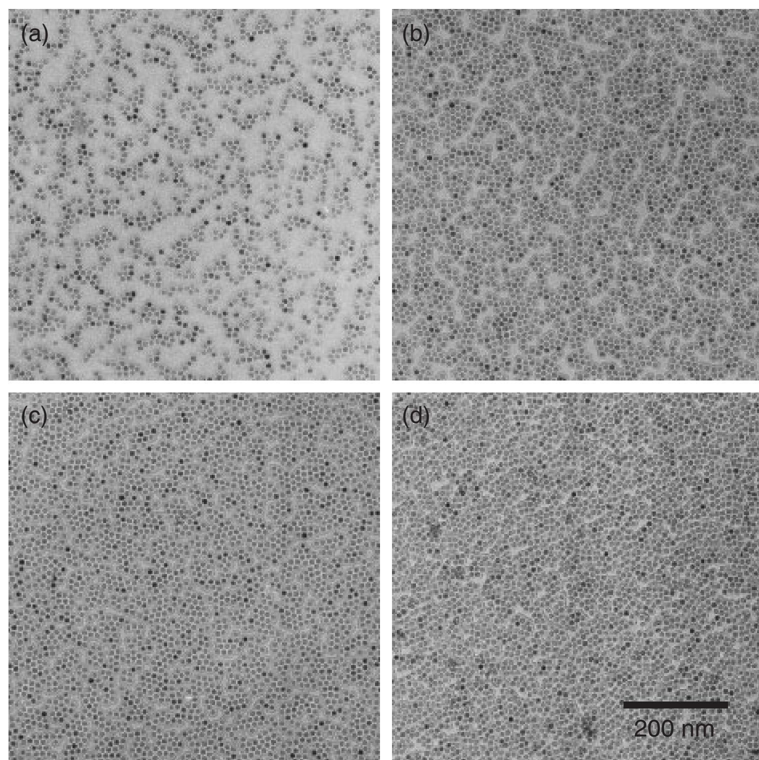

Figure 4. Plan-view TEM bright-field images of the γ-Fe_2O_3 nanoparticles adsorbed on a hydrogen-terminated Si substrate when the number of adsorption steps n is a) 1, b) 5, c) 10, and d) 15 times.

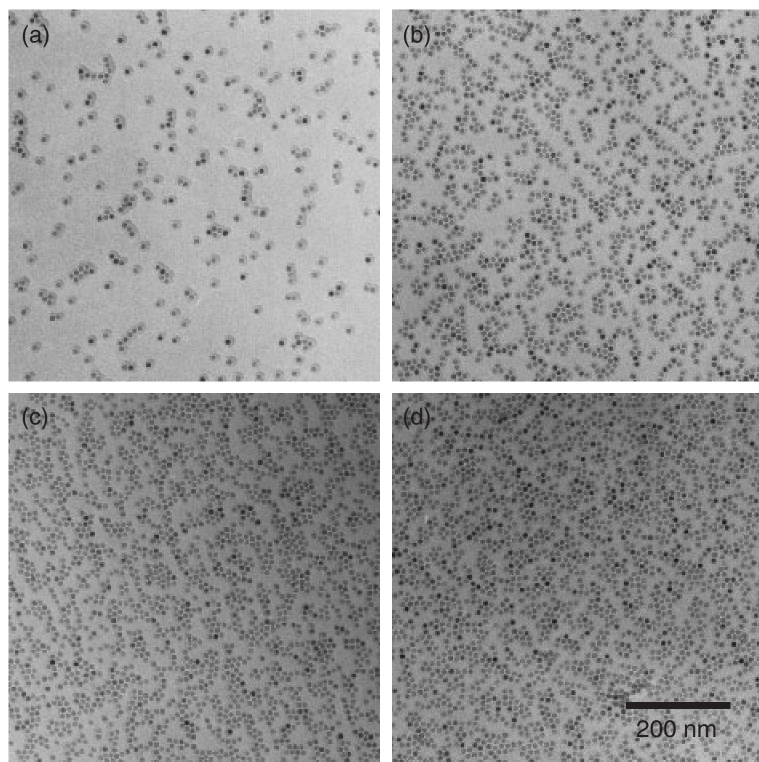

Figure 5. Plan-view TEM bright-field images of the γ-Fe_2O_3 nanoparticles adsorbed on a thermally grown SiO_2 substrate when the number of adsorption steps n is a) 1, b) 5, c) 10, and d) 15 times.

and Figure 5 (on SiO_2). Figure 6 shows a plot of coverage with the number of dipping steps. Indeed, the coverage on Si substrate increases from 0.28 ± 0.01 at $n=1$ to 0.76 ± 0.01 at $n=15$, which corresponds to a spatial density of nanoparticles of 6.1×10^{11} cm^{-2} (the monolayer has a density of 8×10^{11} cm^{-2}). After the first adsorption step ($n=1$, Fig. 4a), the assemblies consist of 1–30 nanoparticles, most of which are either monomers or dimers, depending on the solution concentration (Fig. 1). After repeating the adsorption steps, assemblies cover nearly the whole surface, connected to each other with non-close-packed boundaries (Figs. 4b–d). It should be also noted that the hydrogen-terminated Si surface might be oxidized during the multiple dip-coating process. In order to identify the surface state, we checked the water contact angle of the hydrogen-terminated Si surface before and after dipping in pure octane solvent (without particles or oleic acid), up to 15 times. In addition, the Si surface with native oxide was measured for comparison. It was found that the contact angle gradually decreased from ~77° to ~60° after dipping 15 times. However, the contact angle after multiple-dip coating is still much higher than that of Si substrate with native oxide thereon (~30°). This indicates that the hydrogen-terminated Si surface is not completely oxidized within the time required for dipping 15 times. Similarly, the coverage on SiO_2 substrate increases up to about 0.61 ± 0.006 after repeating the dipping process 15 times, even though the single adsorption coverage is quite low (about 0.08 ± 0.005). The assemblies do not have a completely ordered structure with non-close-packed boundaries between each assembly, unlike those formed by Langmuir–Blodgett method.[17–20] This is thought to result from the small size of the assemblies produced during the first step, but this can be improved by controlling the nucleation and growth of assemblies. In addition, a multilayer is not found even after multiple-adsorption steps, clarifying that the particles adsorb by the interaction between particle and substrate, without aggregation of particles due to stabilization by surfactants.

One of the notable facts about the colloidal assembly is that the inter-particle distance is reduced after evaporation of the solvent. For instance, Giersig and Mulvaney observed the shape of tear in the nanoparticle layer after evaporation of solvent,[44] indicating that the effective area of the nanoparticles shrinks as the solvent is evaporated. Also, Connolly et al. directly measured the inter-particle distance of dodecanethiol-stabilized Ag particles (average particle size: 6.7 nm; extended length of dodecanethiol: 1.5 nm) during the evaporation of solvent using time-resolved small-angle X-ray scattering.[45] According to their results, the inter-parti-

 © 2004 WILEY-VCH Verlag GmbH & Co. KGaA, Weinheim

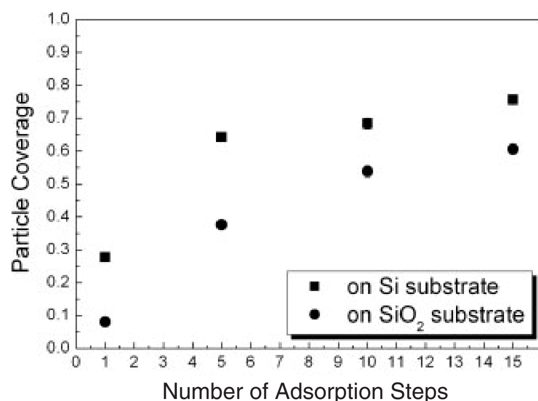

Figure 6. Particle coverage as a function of the number of adsorption steps in the multiple-step dip-coating process.

cle distance decreased by about 10 % after solvent evaporation. If the inter-particle distance of the assemblies are about 10 % larger in solution than in air, the maximum coverage should be around 80 % when the solvent is fully dried. Therefore, the swelling of assemblies in solution possibly prevents further adsorption in solution, and causes the sub-monolayer coverage. Indeed, this can be one of the fundamental limitations to adsorbing particles with 100 % coverage using any kind of wet-chemical technique, such as Langmuir–Blodgett, spin-coating, and dipping processes, when surfactant-stabilized colloidal particles are used. When a large area of self-assembly from solution is obtained, as commonly observed when using the Langmuir–Blodgett technique, it eventually forms cracks as the solvent evaporates due to the areal shrinkage. The degree of shrinkage appears to depend on the relative size of the particles and the surfactant employed.

3. Conclusions

We investigated the adsorption of sterically stabilized nanoparticles on a substrate, which is dependent on the interactions between particle and substrate. The coverage in a single adsorption process was found to be less than 0.5, due to either competitive adsorption between particle and surfactant or to the random sequential-adsorption problem. In order to increase the coverage, we suggest a multiple-adsorption process of repeated dipping of the substrate, followed by drying of the solvent after withdrawing the substrate from the solution. It was experimentally demonstrated that a γ-Fe_2O_3 nanoparticle (10 nm) layer was formed by the multiple-adsorption process, with a coverage of about 0.76 on a hydrogen-terminated Si substrate, and about 0.61 on a thermally grown SiO_2 substrate. These values are larger than the jamming limit (~0.55) in random sequential adsorption.

4. Experimental

Sterically stabilized maghemite (γ-Fe_2O_3) nanoparticles of 10 nm-diameter ($\sigma < 5$ %, measured by high-resolution transmission electron microscopy) were chemically synthesized by decomposition of iron pentacarbonyl ($Fe(CO)_5$) with an oxidizing agent (trimethylamine *N*-oxide, $(CH_3)_3NO$) in a mixture of octyl ether and oleic acid ($C_{18}H_{34}O_2$), and then dissolved in octane (C_8H_{18}) solvent [16]. Unless otherwise noted, all reactions were carried out in a dry argon atmosphere. Octyl ether (99 %), iron pentacarbonyl (99.999 %), and oleic acid (99 %) were used as purchased from Aldrich. Trimethylamine *N*-oxide dehydrate (98 %, Aldrich), was re-dehydrated in vacuum at 90 °C. Octane (96+ %, GC) was purchased from Kanto Chemical.

To prepare monodisperse iron nanoparticles, 0.2 mL of $Fe(CO)_5$ (1.52 mmol) was added to a mixture containing 10 mL of octyl ether and 1.28 g of oleic acid (4.56 mmol) at 100 °C. The resulting mixture was heated to reflux and kept at that temperature for 1 h. During this process, the initial orange color of the solution gradually changed to black. The resulting black solution was cooled to room temperature, and 0.34 g of dehydrated $(CH_3)_3NO$ (4.56 mmol) was added. The mixture was then heated to 130 °C under an argon atmosphere and maintained at this temperature for 2 h, whereupon it formed a brown solution. The reaction temperature was slowly increased to reflux and the reflux continued for 1 h; the color of the solution gradually turned from brown to black. The solution was then cooled to room temperature, and ethanol was added to yield a black precipitate, which was then separated by centrifuging. The resulting black powder can be easily re-dispersed in hydrocarbon solvents, such as hexane, octane, or toluene. During the particle synthesis, the oleic acid encapsulates the particle surface as a stabilizing agent (surfactant), preventing the aggregation of particles in the solution. The hydrophilic head is attached to the particle, while the hydrophobic tail faces the solvent. Therefore, the particles have a hydrophobic character and are well dispersed in nonpolar solvents such as alkane solvents.

The nanoparticle concentration of the γ-Fe_2O_3 colloidal solution was varied from 0.24 to 49×10^{13} cm^{-3} by dispersing a known amount of nanoparticle powder in solvent. The amount of particles in the powder form was analyzed using inductive coupled plasma atomic emission spectroscopy (ICP-AES, ICPS1000IV, Shimadzu). Particles dispersed in octane solvent at those concentrations were found to be macroscopically stable, without aggregation, for more than a year. Three different substrates were used for single adsorption processes: a hydrogen-terminated Si obtained by dipping Si (100) wafers in buffered HF to remove the native oxide; a 50 nm thick Si_3N_4 layer on Si (100) wafer deposited by low-pressure chemical vapor deposition using SiH_2Cl_2 and NH_3 gases at 785 °C; and a 100 nm thick SiO_2 layer on Si (100) thermally grown at 900 °C in an O_2 environment.

The substrates were vertically dipped in a colloidal solution and pulled out at a rate of 0.1 mm s^{-1}, followed by drying in air at room temperature. After evaporation of the solvent, the substrates were capped with an amorphous carbon film to protect the surfaces from mechanical and chemical damage during sample preparation for transmission electron microscopy (TEM) analysis. The morphologies of the nanoparticle assemblies were analyzed using a plan-view TEM (Philips CM20) at an operation voltage of 200 kV. In addition, we have analyzed several samples using scanning electron microscopy as well as TEM, and obtained similar results, which verifies that the assembly was completely protected from damage during TEM sample preparation. The coverage of nanoparticles was measured by counting the number of nanoparticles within four different areas each of 0.5 μm × 0.5 μm. In this article, the coverage was defined as the ratio of the number of adsorbed nanoparticles on the substrate to the theoretical number obtainable in a close-packed nanoparticle monolayer. The particles self-assemble with a hexagonal close-packed array after the drying process, with 2 nm spacing between the particles, indicating a full coverage of particles of 8×10^{11} particles cm^{-2}.

 © 2004 WILEY-VCH Verlag GmbH & Co. KGaA, Weinheim

For the multiple-adsorption process, hydrogen-terminated Si and thermally grown SiO_2 substrates were dipped in a colloidal solution with a concentration of 2.4×10^{13} cm^{-3}, followed by drying the solvent in air. These adsorption steps were repeated 1, 5, 10, and 15 times.

5. Appendix

The Hamaker constant of γ-Fe_2O_3 was calculated by

$$A=\frac{3}{4}kT\left(\frac{\varepsilon_1-\varepsilon_3}{\varepsilon_1+\varepsilon_3}\right)^2+\frac{3h\nu_e}{16\sqrt{2}}\frac{\left(n_1^2-n_3^2\right)^2}{\left(n_1^2+n_3^2\right)^{3/2}} \qquad (2)$$

where $n=\varepsilon^{1/2}=2.63$ (*CRC Handbook of Chemistry and Physics*, 81st ed. (Ed: D. R. Lide), CRC Press, Boca Raton, FL **2000**) and ν_e was typically assumed as 3×10^{15} s^{-1}.

Received: October 13, 2003
Final version: March 5, 2004

[1] D. V. Averin, K. K. Likharev, in *Single Charge Tunneling: Coulomb Blockade Phenomena in Nanostructures* (Eds: H. Grabert, M. H. Devoret), Plenum, New York **1992**, Ch. 9.
[2] *Handbook of Nanostructured Materials and Nanotechnology* (Ed: H. S. Nalwa), Academic, San Diego, CA **2000**.
[3] C. B. Murray, C. R. Kagan, M. G. Bawendi, *Annu. Rev. Mater. Sci.* **2000**, *30*, 545.
[4] A. P. Alivisatos, *Science* **1996**, *271*, 933.
[5] a) T. Hyeon, *Chem. Commun.* **2003**, 927. b) T. Hyeon, Y. Chung, J. Park, S. S. Lee, Y.-W. Kim, B. H. Park, *J. Phys. Chem. B* **2002**, *106*, 6831.
[6] S. Sun, C. B. Murray, *J. Appl. Phys.* **1999**, *85*, 4325.
[7] D. M. Kolb, R. Ullmann, T. Will, *Science* **1997**, *275*, 1097.
[8] M. L. Ostraat, J. De Blauwe, M. L. Green, L. D. Bell, M. L. Brongersma, J. Casperson, R. C. Flagan, H. A. Atwater, *Appl. Phys. Lett.* **2001**, *79*, 433.
[9] S. Tiwari, F. Rana, H. Hanafi, A. Hartstein, E. F. Crabbe, K. Chan, *Appl. Phys. Lett.* **1996**, *68*, 1377.
[10] T.-S. Yoon, K.-B. Kim, *J. Vac. Sci. Technol., B: Microelectron. Nanometer Struct.—Process., Meas., Phenom.* **2002**, *20*, 631.
[11] M. Klimenkov, J. von Borany, W. Matz, R. Grötzschel, F. Herrmann, *J. Appl. Phys.* **2002**, *91*, 10 062.
[12] C. B. Murray, D. J. Norris, M. G. Bawendi, *J. Am. Chem. Soc.* **1993**, *115*, 8706.
[13] V. F. Puntes, K. M. Krishnan, A. P. Alivisatos, *Science* **2001**, *291*, 2115.
[14] C. P. Collier, T. Vossmeyer, J. R. Heath, *Annu. Rev. Phys. Chem.* **1998**, *49*, 371.
[15] B. A. Korgel, D. Fitzmaurice, *Phys. Rev. Lett.* **1998**, *80*, 3531.
[16] T. Hyeon, S. S. Lee, J. Park, Y. Chung, H. B. Na, *J. Am. Chem. Soc.* **2001**, *123*, 12 798.
[17] S. Huang, G. Tsutsui, H. Sakaue, S. Shingubara, T. Takahagi *J. Vac. Sci. Technol., B: Microelectron. Nanometer Struct.—Process., Meas., Phenom.* **2001**, *19*, 2045.
[18] G. Markovich, D. V. Leff, S.-W. Chung, H. M. Soyez, B. Dunn, J. R. Heath, *Appl. Phys. Lett.* **1997**, *70*, 3107.
[19] Q. Guo, X. Teng, S. Rahman, H. Yang, *J. Am. Chem. Soc.* **2003**, *125*, 630.
[20] S. Chen, *Langmuir* **2001**, *17*, 2878.
[21] Y.-K. Hong, H. Kim, G. Lee, W. Kim, J.-I. Park, J. Cheon, J.-Y. Koo, *Appl. Phys. Lett.* **2002**, *80*, 844.
[22] S. Coe, W.-K. Woo, M. Bawendi, V. Bulovic, *Nature* **2002**, *420*, 800.
[23] M. C. Schlamp, X. Peng, A. P. Alivisatos, *J. Appl. Phys.* **1997**, *82*, 5837.
[24] T. Sato, D. G. Hasko, H. Ahmed, *J. Vac. Sci. Technol., B: Microelectron. Nanometer Struct.—Process., Meas., Phenom.* **1997**, *15*, 45.
[25] K. C. Grabar, K. J. Allison, B. E. Baker, R. M. Bright, K. R. Brown, R. G. Freeman, A. P. Fox, C. D. Keating, M. D. Musick, M. J. Natan, *Langmuir* **1996**, *12*, 2353.
[26] D. I. Gittins, A. S. Susha, B. Schoeler, F. Caruso, *Adv. Mater.* **2002**, *14*, 508.
[27] J. Feder, I. Giaever, *J. Colloid Interface Sci.* **1980**, *78*, 144.
[28] N. A. Kotov, I. Dékány, J. H. Fendler, *J. Phys. Chem.* **1995**, *99*, 13 065.
[29] S. Sun, S. Andres, H. F. Hamann, J.-U. Thiele, J. E. E. Baglin, T. Thomson, E. E. Fullerton, C. B. Murray, B. D. Terris, *J. Am. Chem. Soc.* **2002**, *124*, 2884.
[30] L. Motte, E. Lacaze, M. Maillard, M. P. Pileni, *Appl. Surf. Sci.* **2000**, *162*, 604.
[31] R. D. Tilley, S. Saito, *Langmuir* **2003**, *19*, 5115.
[32] G. Y. Onoda, E. G. Linger, *Phys. Rev. A* **1986**, *33*, 715.
[33] J. G. Truong, P. C. Wayner, Jr., *J. Chem. Phys.* **1987**, *87*, 4180.
[34] L. D. Landau, B. G. Levich, *Acta Physicochim. URSS* **1942**, *17*, 42.
[35] *Lange's Handbook of Chemistry*, 15th ed. (Ed: J. A. Dean), McGraw-Hill, New York **1999**.
[36] J. N. Israelachvili, *Intermolecular and Surface Forces*, Academic Press, San Diego, CA **1992**.
[37] D. Bargeman, F. Van Voorst Vader, *J. Electroanal. Chem. Interfacial Electrochem.* **1972**, *37*, 45.
[38] L. Bergström, *Adv. Colloid Interface Sci.* **1997**, *70*, 125.
[39] T. Fried, G. Shemer, G. Markovich, *Adv. Mater.* **2001**, *13*, 1158.
[40] Y. Lu, J. Drelich, J. D. Miller, *J. Colloid Interface Sci.* **1998**, *202*, 462.
[41] G. Ge, L. Brus, *J. Phys. Chem. B* **2000**, *104*, 9573.
[42] P. S. Shah, J. D. Holmes, K. P. Johnston, B. A. Korgel, *J. Phys. Chem. B* **2002**, *106*, 2545.
[43] T.-S. Yoon, S.-H. Park, V. Kim, C. Kwon, K.-B. Kim, B. G. Jung, S.-H. Min, J. Park, T. Hyeon, unpublished.
[44] M. Giersig, P. Mulvaney, *J. Phys. Chem.* **1993**, *97*, 6334.
[45] S. Connolly, S. Fullam, B. Korgel, D. Fitzmaurice, *J. Am. Chem. Soc.* **1998**, *120*, 2969.

 © 2004 WILEY-VCH Verlag GmbH & Co. KGaA, Weinheim